IEEE Access
Multidisciplinary | Rapid Review | Open Access Journal

Received April 20, 2022, accepted May 6, 2022, date of publication May 13, 2022, date of current version May 19, 2022.

Digital Object Identifier 10.1109/ACCESS.2022.3174856

Influence of Shed Shape on Direct-Current Pollution Flashover Voltage and Pressure Decrease Exponent

JIAN LI[1,2,3], ZHONG WANG[3], XIAOBO MENG[4], AND LIMING WANG[5], (Senior Member, IEEE)

[1]NARI Group Corporation Ltd., Nanjing 211106, China
[2]Wuhan NARI Ltd. Liability Company, State Grid Electric Power Research Institute, Wuhan 430074, China
[3]College of Electrical Engineering, Sichuan University, Chengdu 610065, China
[4]School of Mechanical and Electrical Engineering, Guangzhou University, Guangzhou 510006, China
[5]Tsinghua Shenzhen International Graduate School, Tsinghua University, Shenzhen 518055, China

Corresponding authors: Zhong Wang (zhongwang1986@126.com) and Xiaobo Meng (mengxiaobo2008@sina.com)

This work was supported in part by the GuangDong Basic and Applied Basic Research Foundation under Grant 2021A1515110568.

ABSTRACT This study investigated the influencing mechanisms of shed shape on direct-current pollution flashover voltage and pressure decrease exponent through artificial pollution tests on a glass experimental model in Beijing (50 m altitude) and Tibet (4300 m altitude). Arc development before the flashover was quantitatively recorded using a high-speed camera. Three arc development modes along the pollution surface or in the inter-shed space were then extracted through arc development analysis. The occurrence probabilities of the three arc modes under various shed overhangs, altitudes, and shed spacings were analyzed. Mode probability was used to interpret the decreasing flashover voltage gradient with increasing shed overhang and decreasing shed spacing. Research indicates that pressure decrease exponent rises with shed overhang increase, as explained from the perspective of arc development probability. The quantitative relation between leakage distance efficiency and pressure decrease exponent was theoretically derived, and its validity was proven by comparing the calculated with the measured.

INDEX TERMS Arc development probability, direct-current pollution flashover voltage, insulator shed shape, leakage distance efficiency, pressure decrease exponent.

I. INTRODUCTION

Ultra-high-voltage direct-current (UHVDC) power transmission projects in China are increasing. A few overhead transmission lines of these projects pass through heavily contaminated and high-altitude areas. The pollution flashover problem for glass/porcelain insulators at high altitudes is of great concern. The influences of contamination and altitude (or air pressure) on the pollution flashover characteristics of multiple shed shapes of insulators have been considerably researched [1]–[37]. However, most of these studies are engineering tests rather than investigations on the microscopic influencing mechanism of insulator shed shape on its pollution flashover voltage. The influencing degree of altitude on the insulator pollution flashover voltage is related to the shed shape of the insulator [11], [14], [23], [25], [26], [29], [38]–[41]. A complex shed shape of the insulator is believed to correspond to a significant decrease degree of the pollution flashover voltage with the increase in altitude [11], [42].

Early in 1972, the mathematical relationship between the pollution flashover voltage and the altitude was proposed, and its pressure decrease exponent was defined [43]. The influence degree of air pressure on the pollution flashover voltage was characterized by air pressure decrease exponent. The pressure decrease exponents of a standard form insulator were separately determined to be 0.4, 0.35, and 0.5 for positive DC, negative DC, and AC, respectively, according to numerous artificial pollution tests [38]. With that, a large number of investigations on the pressure decrease exponent were conducted through the artificial pollution test in the actual high-altitude areas and a climatic chamber [11], [14], [23], [25], [26], [29], [39]–[41].

The associate editor coordinating the review of this manuscript and approving it for publication was Arpan Kumar Pradhan.

Results indicated that various shed shapes of insulators owned different pressure decrease exponents. However, the essential relationship between the pressure decrease exponents and the insulator shed shape remains unclear.

Hoch and Swift [44] stated that the lowering arc volt-ampere characteristic was not the only factor in the decline of flashover voltage in the high-altitude area. Based on their analysis of the influence of air density on the flashover voltage, flashover also resulted from the combined action of arc development along the surface and air breakdown at low pressure. The contributions of the two mechanisms were also different at various shed shapes and applied voltages. However, this innovative work on the influence mechanism of air pressure failed to clearly elucidate the actions of these two mechanisms and provide the method of determining their respective contributions. Therefore, this work has no evident guiding significance for designing outdoor insulation. Cheng and Nour [45], [46] found that the insulator ridge structure affected the arc development path between ridges and provided the empirical expression of the leakage distance efficiency by examining the effect of the insulator ridge structure on DC pollution flashover voltage. Rizk [47] indicated that the arc development between ridges was not only related to the insulator structure but also the ratio of the voltage gradient required for the streamer propagation to the flashover voltage gradient. He also improved the empirical expression of the leakage distance efficiency by involving the effect of air pressure based on Cheng and Nour's work. The introduction of the voltage gradient ratio was a considerable improvement. The enhanced expression could also reflect the effect of air pressure on the flashover voltage of various shed shapes of insulators, but it had no precise physical mechanism. The two preceding expressions were both proposed based on the observations on arc development, but both lacked a quantitative analysis of arc development. Thus, determining the effect of arc development on the leakage distance efficiency from these two expressions was difficult. Zhang *et al.* observed that the partial arcs included two main parts, namely air gap arc and surface arc, from the DC flashover process of the polluted insulator at high altitude; on this basis, a new physical model explaining the pollution flashover mechanism at high altitude was introduced using a resistance series circuit consisting of a surface arc, an air-gap arc and the residual pollution layer of the insulator string. They then stated that the pressure decrease exponent depended on the length ratio of the air-gap arc to the surface arc during the flashover process through solving the model, and that the dominating reason of different exponents was the partial arc fluttering degree difference for various shed shapes of insulators. However, this research only considered two extreme cases, including that the partial arcs are all surface arcs and that the partial arcs are all air-gap arcs, and did not give the influence laws of shed shape on the occurrence probabilities of these two forms of partial arcs and the relative amount of these two arcs on the pressure decrease exponent [11], [12].

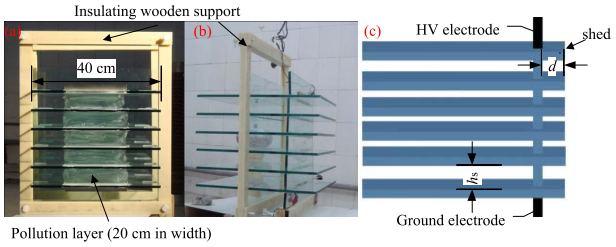

FIGURE 1. Experimental model: (a) front view, (b) side view, and (c) schematic diagram (d: shed overhang, h_S: shed spacing).

In this paper, a simplified experimental model with a similar structure to the insulator was self-designed to quantificationally and expediently investigate the influencing mechanism of shed shape on the pollution flashover voltage and its gradient, the development probabilities of various forms of partial arcs and the pressure decrease exponent through the artificial pollution tests on this model in Beijing (50 m altitude) and Tibet (4300 m altitude). The arc development before the flashover of various shed sizes of experimental models at these two altitudes was quantitatively recorded, and the arc development in the inter-shed space was analyzed from the perspective of probability statistics. On this basis, the relationship between the leakage distance efficiency and the development probabilities of various partial arcs was examined, and the influencing mechanism of shed shape on the pressure decrease exponent was interpreted.

II. EXPERIMENTAL SET-UP

Fig. 1 shows the self-designed experimental model. Unlike an actual porcelain/glass insulator, this simple model helps in quantitatively analyzing the relationships among arc development characteristics, pollution flashover, and model parameters. As shown in the figure, six large plate glasses (8 mm thickness and 40 cm width) were uniformly spaced and horizontally inserted into the grooves of an aided insulating wooden support. Seven small plate glasses were also vertically inserted separately into the space between any two adjacent large plate glasses. The joints between the large and small plate glasses were glued and sealed using glass cement to prevent the formation of mini air gaps at the joints. Thus, some glass sheds with the preset shed overhang d and shed spacing h_s were formed. The small plate glasses were not precisely located in the middle of the inter-shed space to facilitate flashover occurrence only at the side with a small leakage distance.

The solid layer method was used to pollute the experimental model. A specific slurry comprising NaCl, kaolin powder, and distilled water was uniformly coated onto the glass surface (the width of the pollution area was 20 cm in the middle). China's pollution degree was heavy, the pollution layer had an equivalent salt deposit density (ESDD) of 0.05 mg/cm^2 and a non-soluble deposit density (NSDD) of 1.0 mg/cm^2 [1], [2]. The amount of NaCl and kaolin was

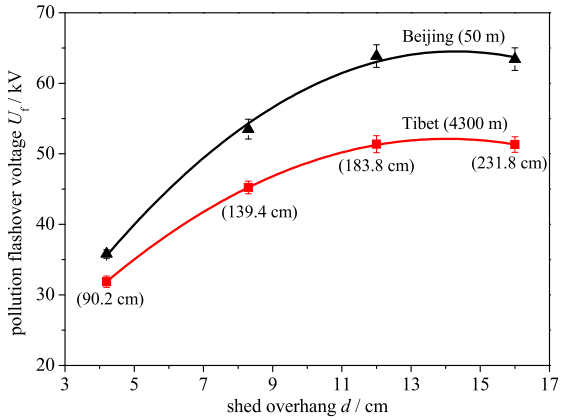

FIGURE 2. Variation of pollution flashover voltage U_f with shed overhang d at two altitudes (50 and 4300 m in Beijing and Tibet, respectively; h_s = 7 cm).

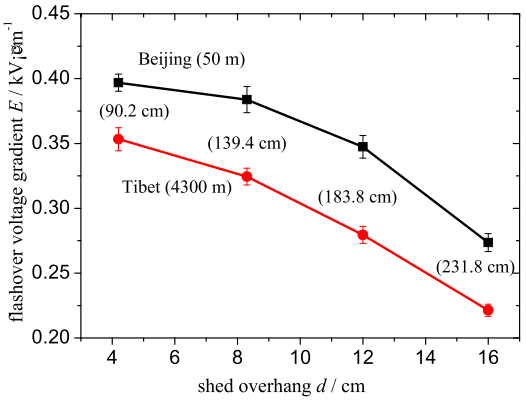

FIGURE 3. Variation of flashover voltage gradient gU_f with shed overhang d at two altitudes (50 and 4300 m in Beijing and Tibet, respectively; h_s = 7 cm).

obtained according to the surface area of the experimental model by multiplying ESDD and NSDD. After the turbid liquid was prepared with distilled water, it was evenly coated on the surface of the experimental model. A certain amount of distilled water was uniformly coated on the contamination layer after drying. The wetting method has the advantages of small test sample dispersity, convenient operation, uniform wetting, and avoidance of visibility reduction (fog wetting may reduce visibility). These advantages are beneficial for the clear recording of the arc development process by a high-speed camera.

The insulating wooden support was removed after the contamination layer wetting, and then a DC voltage was applied to the polluted glass experimental model. The 50% pollution flashover voltage was determined according to the up-and-down method similar to that in the artificial pollution test [48], [49]. Slightly different, an expected voltage was preset, and the silicon control of the DC source system was then switched on, thus immediately applying the voltage to the glass model due to the high response speed of the silicon control. The pollution layer was recoated and wetted every time before voltage application due to the specificity of the preceding wetting method mentioned.

III. POLLUTION FLASHOVER VOLTAGE

A. INFLUENCE OF SHED OVERHANG

Fig. 2 shows the variation of pollution flashover voltage U_f with the shed overhang d at two altitudes (50 and 4300 m in Beijing and Tibet, respectively). The air pressure of Beijing is 101kPa, and that of Tibet is 59.3kPa. As shown in the figure, pollution flashover voltage initially increases and then slightly decreases with the increase in shed overhang. The method of most minor square polynomial fitting is used to fit the experimental data. The fitting gives Equations (1) and (2) a correlation coefficient of 0.99 for Beijing and 1 for Tibet. The close to 1 coefficient indicates that the quadratic polynomial is suitable to fit the relationship between pollution flashover voltage and shed overhang. Maximizing U_f in Equations (1) and (2) can provide optimal shed overhangs of 14.3 cm for Beijing and 14 cm for Tibet. Specifically, a small shed overhang is required to reach the peak flashover voltage at a high altitude.

$$\begin{cases} U_f = -0.2847d^2 + 8.1356d + 6.4017 \text{ (Beijing)} & (1) \\ U_f = -0.2110d^2 + 5.9139d + 10.7374 \text{ (Tibet)} & (2) \end{cases}$$

Fig. 3 presents the variation of pollution flashover voltage gradient U_f with shed overhang d at two altitudes (50 and 4300 m in Beijing and Tibet, respectively). The flashover voltage gradient results from the flashover voltage divided by the leakage distance, which is labeled in a round bracket of the figure. The flashover voltage gradient decreases at an increasing rate as the shed overhang increases.

The arc development before the flashover for various shed overhangs is recorded using a high-speed camera (FASTCAM ultima 1024) at a rate of 1000 fps. Fig. 4 illustrates that for any shed overhang, the arc initiates at the shed root of the shed's lower surface, where the dry band easily forms and then develops toward two ends. The arc is more evident at the top sheds than at the bottom sheds. The arc development difference between the top and bottom sheds may be attributed to the randomness of the dry band formation or the non-uniformity of the pollution coating.

The arc is notably different for various shed overhangs. The arc develops tightly along the shed surface until the flashover in the case of the 4.2 cm shed overhang (Fig. 4a), and the formation of a steady inter-shed arc is difficult. As the shed overhang increases to 8.3 cm, a stable inter-shed arc is formed, and the time necessary to reach the flashover increases. The stable inter-shed arc marked with a rectangular wireframe in Fig. 4b moves outward as time passes. The length of the inter-shed arc is shorter than that of the arc along the shed surface, and this shortening degree increases as the arc moves outward, resulting in a low arc voltage. Therefore, a slight pollution flashover voltage gradient and the efficiency of leakage distance for a large shed overhang can be attributed to the formation and movement outward of the inter-shed arc.

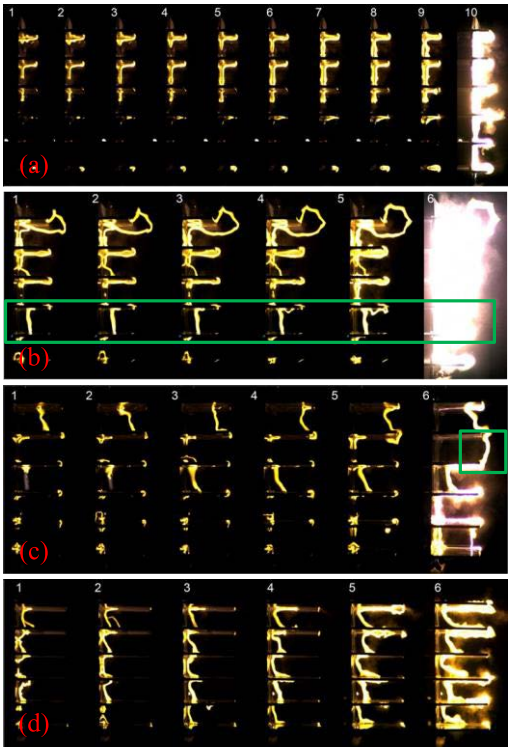

FIGURE 4. Arc development prior to the flashover for various shed overhangs: (a) $d = 4.2$ cm, (b) $d = 8.3$ cm, (c) $d = 12$ cm, and (d) $d = 16$ cm ($h_s = 7$ cm). The interval time is 40ms.

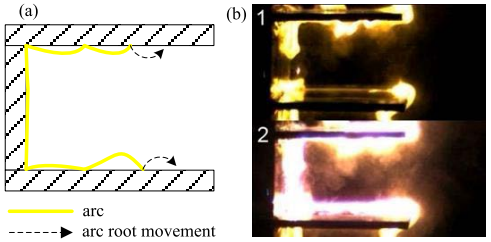

FIGURE 5. Mode 1 (along surface arc): (a) schematic diagram and (b) photo, inter-frame space 1 ms.

The formation and movement outward of the inter-shed arc become evident as the shed overhang increases. Meanwhile, another arc development mode appears. This mode is the direct bridging of two adjacent shed edges by the arc, which is marked with a rectangular wireframe in Fig. 4c. The arc length further shortens, resulting in the lowering pollution flashover voltage gradient and efficiency of leakage distance similar to the mode in Fig. 4b.

Three arc development modes are extracted through numerous experiments and observations as follows:

Mode 1: The arc along the surface in Fig. 4a. The mode is defined as along surface arc; the length-increasing arc floating belongs to this mode. This arc mode is characterized by the absence of overall movement outward, a short duration (The duration is lower than 100ms), instability, and easy extinguishment (Fig. 5).

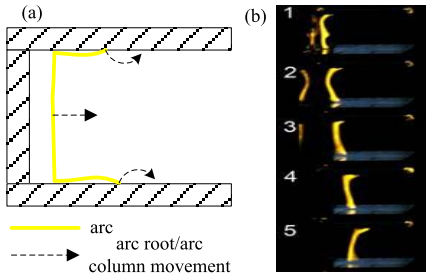

FIGURE 6. Mode 2 (surface bridging arc): (a) schematic diagram and (b) photo, inter-frame space 80 ms.

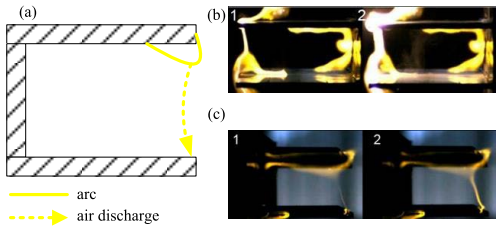

FIGURE 7. Mode 3 (edge bridging arc): (a) schematic diagram, (b) photo, upward bridging, inter-frame space 1 ms, and (c) photo, downward bridging, inter-frame space 1 ms.

Mode 2: This mode involves the arc bridging the upper and lower surfaces of two adjacent sheds and moving outward to separate from the vertical surface (Fig. 4b). This mode is defined as a surface bridging arc. It has the characteristics of a relatively fixed arc length, a long duration (The duration is greater than 100ms), stability, and difficult extinguishment (Fig. 6).

Mode 3: This mode involves the arc directly bridging two adjacent shed edges (Fig. 4c). The inter-shed arc moves toward the adjoining shed, which leads to the breakdown of the inter-shed air gap, thereby forming an arc directly bridging the two neighboring sheds. This mode is defined as an edge bridging arc. It has the characteristics of occasional occurrence, short duration, and easy appearance at the shed edge. However, this arc mode generally becomes relatively stable and difficult to extinguish after bridging the two adjacent sheds (Fig. 7).

The occurrence probabilities of the three arc modes were calculated to interpret the decrease in pollution flashover voltage gradient with the increase in shed overhang (Fig. 3). The occurrence probability P_i of the i-th arc developing mode is defined as

$$P_i = \frac{\sum_{j=1}^{j=n} N_{ij}}{5n} \tag{3}$$

where $i = 1, 2$, and 3 correspond to Modes 1, 2, and 3, respectively; n is the flashover times in many repeated experiments; N_{ij} is the number of shed–shed gaps where the arc develops in the i-th arc mode for the j-th flashover; and 5n is the total number of gaps due to five shed–shed gaps; that is, six sheds

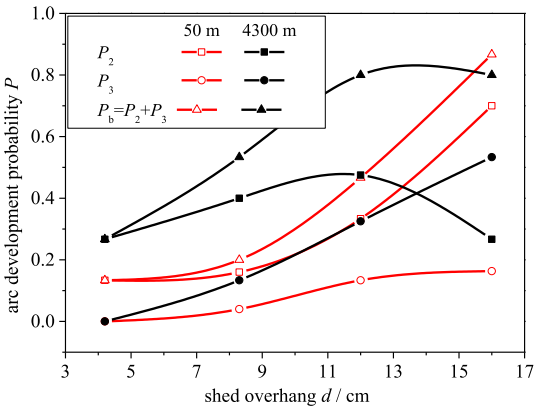

FIGURE 8. Variation of the occurrence probabilities of modes 2 and 3 of the arc with shed overhang at two altitudes: 50 m (Beijing) and 4300 m (Tibet), ($h_s = 7$ cm).

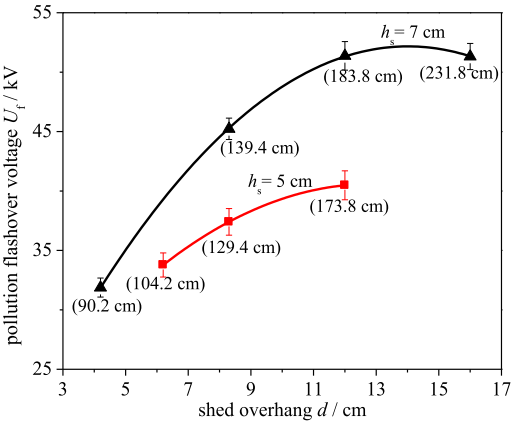

FIGURE 9. Dependence of pollution flashover voltage on shed overhang at two shed spacings (h_s) at 4300 m altitude (Tibet).

for every kind of shed overhang of the test sample model (Fig. 1c). The flashover times are assumed to be larger than five for every test model; that is, the sampling size is $5n > 25$. The relationship among P_1, P_2, and P_3 is as follows:

$$P_1 + P_2 + P_3 = 1 \tag{4}$$

Fig. 8 shows the variation of occurrence probabilities of Modes 2 and 3 of arcs with shed overhang at two altitudes, 50 m (Beijing) and 4300 m (Tibet). The arc bridging probability P_b is the sum of the arc surface bridging probability P_2 (Mode 2) and the arc edge bridging probability P_3 (Mode 3). As shown in Fig. 8, in the case of altitude 50 m, P_2 and P_3 increase with shed overhang, and the former rapidly grows. P_b increases from 0.13 to 0.87 as the shed overhang increases from 4.2 cm to 16 cm, and P_2 considerably contributes to P_b. The increasing difference between $P_2 - P_3$ with the rise in shed overhang means that Mode 2 of the arc becomes dominant before the flashover as the shed overhang increases. According to (3), the probability of P_1 of the arc developing along the surface decreases from 0.87 to 0.13. The increase in P_b and decrease in P_1 indicate that greater leakage distance is bridged by the arc with the increase in shed overhang, which leads to the decline in flashover voltage gradient. An increasing leakage distance due to increasing shed overhang and decreasing flashover voltage gradient prevents the increase in flashover voltage (the product of both) with shed overhang; for example, the approach of the flashover voltage at 12 cm to that at 16 cm in Fig. 2.

The arc bridging probability P_b at a high altitude of 4300 m is larger than that at a low altitude of 50 m. It increases with the shed overhang until 0.8 at 12 cm, which is closes to 0.87 at the 16 cm shed overhang at a low altitude of 50 m. This finding proves the validity of the viewpoint that the arc effortlessly floats at a high altitude from the angle of probability statistics.

The variation of the arc development probability with shed overhang at altitude 4300 m slightly differs from that in altitude 50 m. The arc surface bridging probability P_2 (Mode 2) initially increases and decreases with the rise in shed overhang and maximizes at 12 cm at high altitude. By contrast, the arc edge bridging probability P_3 (Mode 3) always increases as the shed overhang increases and exceeds P_2 at 16 cm. This probability excess at a large shed overhang means that Mode 3 of the arc becomes dominant before the flashover at a large shed overhang because of the easy air breakdown at high altitudes. The increase in P_b and decrease in P_1 indicate that greater leakage distance is bridged by the arc with the increase in shed overhang, which leads to the decrease in flashover voltage gradient.

The difference in arc development before the flashover for various shed overhangs is qualitatively illustrated through the photos in Fig. 4. By contrast, the arc development difference is quantitatively explained using the arc development probability provided in Fig. 8.

B. INFLUENCE OF SHED SPACING

Fig. 9 shows the dependence of pollution flashover voltage on shed overhang at two shed spacings (h_s) at 4300 m altitude (Tibet). The figure shows that a large shed spacing results in a high flashover voltage in the case of the same shed overhang. The relationship of the both is quantified using a quadratic polynomial fitting on the experimental data. The fitting provides Equation (5) and (6) with a correlation coefficient of 0.99 for $h_s = 5$ cm and 1 for $h_s = 7$ cm. The maximal flashover voltage U_f corresponds to the shed overhang d of 12.8 cm for $h_s = 5$ cm and 14 cm for $h_s = 7$ cm. This finding means that a large shed spacing corresponds to a large optimal shed overhang.

$$\begin{cases} U_f = -0.1543d^2 + 3.9644d + 15.1242 \ (h_s = 5 \text{ cm}) & (5) \\ U_f = -0.2110d^2 + 5.9139d + 10.7374 \ (h_s = 7 \text{ cm}) & (6) \end{cases}$$

Fig. 10 shows the dependence of flashover voltage gradient on shed overhang at two shed spacings (h_s) at 4300 m altitude (Tibet). The figure shows that a large shed spacing corresponds to a high flashover voltage gradient in the case of the same shed overhang, and the gradient difference for the

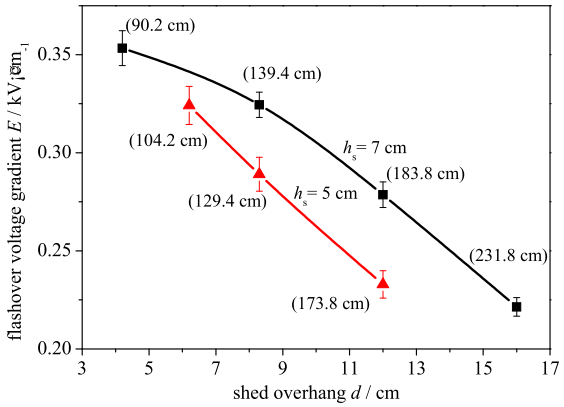

FIGURE 10. Dependence of flashover voltage gradient on shed overhang at two shed spacings (h_s) at 4300 m altitude (Tibet).

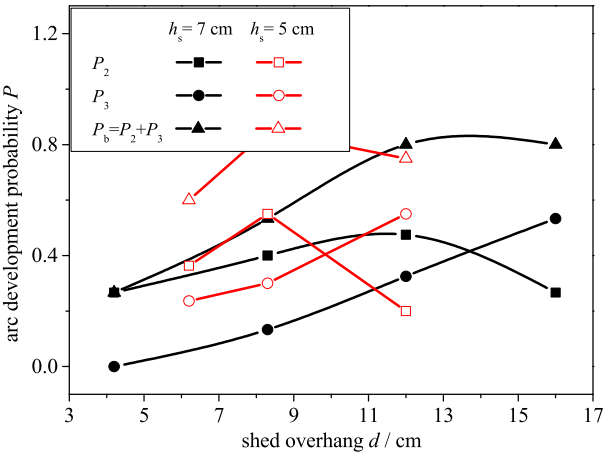

FIGURE 11. Variation of the development probabilities of modes 2 and 3 of the arc with shed overhang at two shed spacings (h_s) at 4300 m altitude.

two shed spacings increases with the rise in shed overhang. This finding indicates that leakage distance has a lower efficiency for a small shed spacing than a large one in the case of a given shed overhang. The leakage distance efficiency rapidly decreases as the shed overhang increases for a small shed spacing, thus leading to a small optimal shed overhang calculated using Equations (5) and (6).

The arc development probabilities of the three arc modes were calculated to explain the decrease of leakage distance efficiency with the increase of shed overhang. Fig. 11 shows the variation of the development probabilities of Modes 2 and 3 of the arc with shed overhang at two shed spacings (h_s) at 4300 m altitude. The arc bridging (Modes 2 and 3), especially the arc edge bridging (Mode 3), weakens the action of leakage distance and then lowers its efficiency. As shown in Fig. 11, the arc edge bridging probability P_3 increases with the rise in shed overhang, leading to a decrease in flashover voltage gradient. A small shed spacing corresponds to a large arc bridging probability P_b, especially P_3. Therefore, the flashover voltage gradient for a small shed spacing is reduced (Fig. 10).

IV. EFFICIENCY OF LEAKAGE DISTANCE

The experiments show that shed overhang, shed spacing, and altitude all influence the arc development. Hence, the efficiency of leakage distance is determined by these three parameters. Leakage distance efficiency is defined as

$$\eta(d, h_s, p) = \frac{E(d, h_s, p)}{E_0(p)} \tag{7}$$

where $E\,(d, h_s, p)$ is the flashover voltage gradient at the shed overhang d, shed spacing h_s, and air pressure p; and $E_0(p)$ is the flashover voltage gradient at the air pressure p in the case of the arc developing entirely along the surface. $E_0(p)$ is obtained using the following expression:

$$E_0(p) = E_0(p_0)(\frac{p}{p_0})^{m_E} \tag{8}$$

where $E_0(p_0)$ is the flashover voltage gradient at the air pressure p_0 in the case of the arc developing entirely along the surface, $E_0(p_0) = 0.397$ kV/cm; and m_E is the pressure decrease exponent of the flashover voltage gradient. The decrease in flashover voltage gradient at the high altitude is mainly caused by the lowering of the volt-ampere characteristics of the arc when it develops entirely along the surface. m_E is experimentally determined as 0.15 based on the plane triangular polluted glass sample in our previous work [50].

Fig. 12 is the variation of leakage distance efficiency η with arc development probability P at altitudes 50 and 4300 m. η is calculated using the flashover voltage gradient in Fig. 3 and 10 according to Equations (7) – (8), and P (P_2, P_3) is derived from Fig. 8 and 11. As shown in Fig. 12, the efficiency η generally decreases as P_2 and P_3 increase at the altitude of 50 m and P_3 increases at the altitude of 4300 m. However, qualitatively determining the relationship between η and P_2 at the latter altitude is difficult. The quantitative relationship between η and P was obtained using multivariate regression analysis. The maximal regression error is 0.75% for 50 m and 6.06% for 4300 m. The small error indicates that η has a linear regression relationship with P_2 and P_3 (Equations 9 and 10).

$$\begin{cases} \eta = -0.4799P_2 - 0.2018P_3 + 1.0588 \;\; 50 \text{ m (Beijing)} & (9) \\ \eta = -0.0279P_2 - 0.6722P_3 + 1 \;\; 4300 \text{ m (Tibet)} & (10) \end{cases}$$

Equation (9) and (10) is generalized as

$$\eta = -k_2P_2 - k_3P_3 + C \tag{11}$$

where k_2 ($\geq$0) and k_3 ($\geq$0) are the influence coefficients of the surface bridging arc (Mode 2) and edge bridging arc (Mode 3) on the leakage distance efficiency, respectively, and C is constant. η is 1 when the arc develops completely along the surface, namely, $P_2 = P_3 = 0$; hence, $C = 1$. Equation (8) is written as follows:

$$\eta = -k_2P_2 - k_3P_3 + 1 \tag{12}$$

k_2 and k_3 are related to the altitude by comparing Equations (9) - (12). At the low altitude, a large k_2 and a small k_3

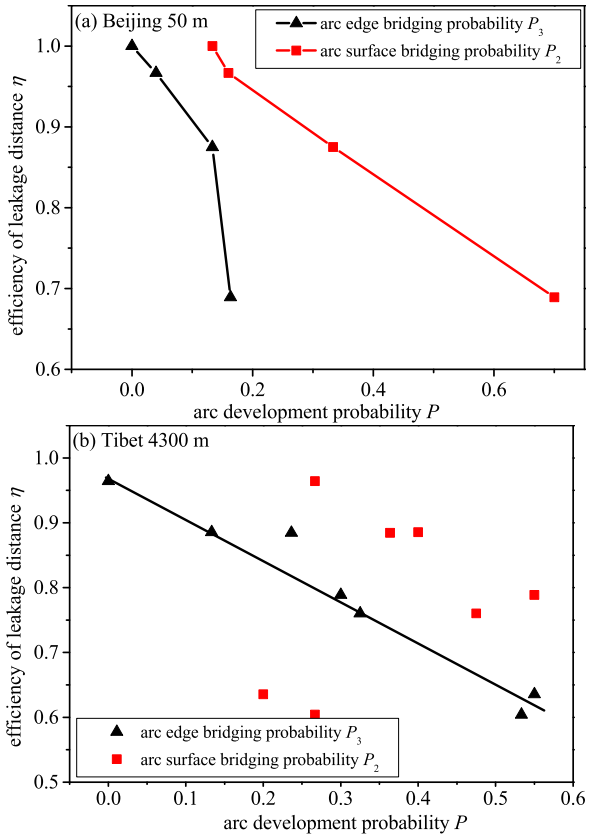

FIGURE 12. Variation of leakage distance efficiency η with arc development probability at altitudes 50 and 4300 m.

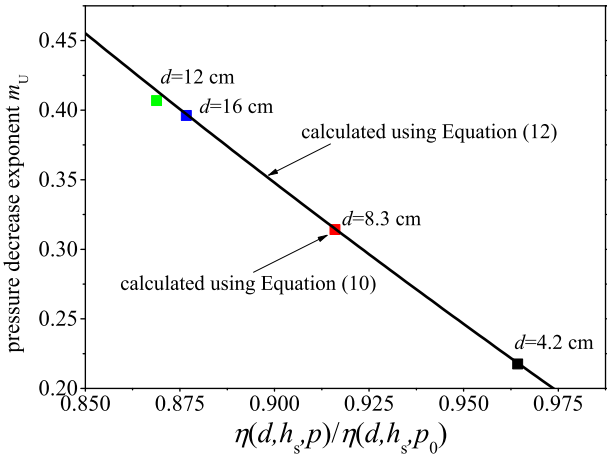

FIGURE 13. Pressure decrease exponents m_U at various shed overhangs d calculated using the two preceding methods mentioned. (p = 4300 m, p_0 = 50 m, h_s = 7 cm).

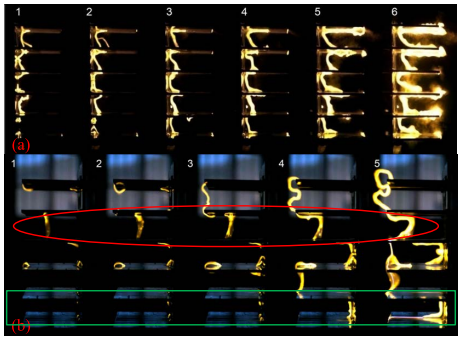

FIGURE 14. Arc development before the flashover at the two altitudes of 50 and 4300 m in the case of 16 cm shed overhang (h_s = 7 cm, inter-frame space 40 ms): (a) 50 m, Beijing; (b) 4300 m, Tibet. The interval time is 40ms.

indicate that the surface bridging arc (Mode 2) is the main factor affecting the leakage distance efficiency. In contrast, at the high altitude, a small k_2 and a large k_3 mean that the edge bridging arc (Mode 3) is the dominant factor affecting the leakage distance efficiency. Moreover, k_2 and k_3 are both dependent on the shed shape, contamination, and wetting.

V. PRESSURE DECREASE EXPONENT

The relationship between pollution flashover voltage and air pressure is expressed as

$$U_f(d, h_s, p) = U_f(d, h_s, p_0)(p/p_0)^{m_U} \quad (13)$$

where $U_f(d, h_s, p)$ and $U_f(d, h_s, p_0)$ are respectively the flashover voltages at the air pressure p and p_0 (=101.3 kPa) for a given shed overhang d and shed spacing h_s, and m_U is the pressure decrease exponent of the flashover voltage.

In the case of a given shed overhang d and shed spacing h_s, Equation (14) is obtained according to Equation (7).

$$\frac{U_f(d, h_s, p)}{U_f(d, h_s, p_0)} = \frac{E(d, h_s, p)}{E(d, h_s, p_0)} = \frac{E_0(p)\eta(d, h_s, p)}{E_0(p_0)\eta(d, h_s, p_0)} \quad (14)$$

According to Equations (8), (13), and (14), the relationship between the pressure decrease exponent m_U and the leakage distance efficiency η is written as

$$(\frac{p}{p_0})^{m_U} = \frac{\eta(d, h_s, p)}{\eta(d, h_s, p_0)}(\frac{p}{p_0})^{m_E} \quad (15)$$

Thus, the pressure decrease exponent m_U of the flashover voltage can be calculated using Equation (15) and the ratio of the leakage distance efficiencies at the air pressure p and p_0.

The pressure decrease exponent can be calculated using the flashover voltages at the altitudes 50 and 4300 m in Fig. 2 according to Equation (13) and the leakage distance efficiency ratio at the two altitudes according to Equation (15). Fig. 13 shows the pressure decrease exponents m_U at various shed overhangs d calculated using the two preceding methods. Fig. 13 indicates that the calculated pressure decrease exponents m_U using Equation (13) precisely on the $m_U - \eta(p) / \eta(p_0)$ curve determined by Equation (15) are within experimental error. This agreement means that Equation (15) can be used to characterize the relationship between the pressure decrease exponent m_U and the leakage distance efficiency ratio.

Fig. 13 shows that the general increase in pressure decrease exponent with the rising shed overhang d indicates that the flashover voltage rapidly decreases with the altitude rising at a large shed overhang. The mechanism is explained as follows. Fig. 14 shows the arc development before the flashover

at the two altitudes of 50 and 4300 m in the case of a 16 cm shed overhang. As shown in Fig. 14b, in the case of high altitude, the presence of along surface arc (Mode 1, marked with a rectangular wireframe) and surface bridging arc (Mode 2, marked with an ellipse) is slightly evident, while the edge bridging arc (Mode 3) appears in the three others shed–shed gaps. The arc development is different at the low and high altitudes. The arc development difference between the two altitudes (e.g., additional edge bridging arc at high altitude) is expected to decrease the flashover voltage at high altitude. In Fig. 8, the arc bridging probability P_b, especially the arc edge bridging probability P_3, increases with the shed overhang d, and P_3 rapidly grows and is large at the high altitude. The large P_3 indicates the appearance of an additional edge bridging arc in the shed–shed gaps. Therefore, the pressure decrease exponent increases along the shed overhang. As shown in Equation (15), the pressure decrease exponent m_U has a definite relationship with the leakage distance efficiency ratio. Equations (9) and (10) indicate that leakage distance efficiency η has a linear variation with the arc development probability P. This finding means that m_U is determined by P, namely, the arc development mode. Therefore, the arc development probability difference for various shed overhangs results in the increase of pressure decrease exponent m_U with the increase of shed overhang.

VI. CONCLUSION

In this research, the influencing mechanisms of shed shape on direct-current pollution flashover voltage and pressure decrease exponent were studied through artificial pollution tests on a simplified self-designed glass experimental model in Beijing (50 m altitude) and Tibet (4300 m altitude). The results led to the following conclusions:

Pollution flashover voltage initially increases and then slightly decreases with the rise of the shed overhang. The flashover voltage is considered a quadratic polynomial of the shed overhang, and a small shed overhang is required to reach the maximum flashover voltage at a high altitude. A large shed spacing results in a high flashover voltage for a given shed overhang. Furthermore, a large shed overhang is necessary to reach the maximum flashover voltage at a large shed spacing.

Flashover voltage gradient decreases at an increasing rate as the shed overhang rises at high and low altitudes, resulting from greater bridged leakage distance by the arc with the increase of shed overhang.

A small shed spacing corresponds to a low flashover voltage gradient for a given shed overhang, resulting from a greater bridged leakage distance by the arc in this case. The gradient difference for the large and small shed spacings increases with the shed overhang.

Overall, the pressure decrease exponent increases as the shed overhang rises, resulting from greater bridged leakage distance by the arc with the increase of shed overhang at high altitude.

Only three arc development modes occur, including along surface arc (Mode 1), surface bridging arc (Mode 2), and edge bridging arc (Mode 3) along the pollution layer surface or in the inter-shed space. Modes 2 and 3 of the arcs reduce the leakage distance efficiency. The probability of every arc development mode is related to the shed overhang, altitude, and shed spacing. Overall, Modes 2 and 3 of arc occur more at a high altitude, as well as at a large shed overhang and a small shed spacing. Mode 2 is the dominant arc mode at low altitude, while Mode 3 is the dominant arc mode at high altitude.

The pressure decrease exponent has a precise mathematical relationship with leakage distance efficiency. This efficiency has a linear regression relation with arc development probability, and the linear regression coefficients are different at various altitudes. The pressure decrease exponent is essentially determined by the relative extent of the three arc development modes.

REFERENCES

[1] F. Zhang, J. Zhao, L. Wang, and Z. Guan, "Experimental investigation on outdoor insulation for DC transmission line at high altitudes," *IEEE Trans. Power Del.*, vol. 25, no. 1, pp. 351–357, Jan. 2010.

[2] Z. Fuzeng, W. Xin, L. Biao, W. Liming, and G. Zhicheng, "Influence of angles of V-strings on DC flashover characteristics of polluted insulators in high altitude areas," in *Proc. IEEE Conf. Electr. Insul. Dielectr. Phenomena*, Oct. 2006, pp. 449–452.

[3] X. Jiang, J. Yuan, L. Shu, Z. Zhang, J. Hu, and F. Mao, "Comparison of DC pollution flashover performances of various types of porcelain, glass, and composite insulators," *IEEE Trans. Power Del.*, vol. 23, no. 2, pp. 1183–1190, Apr. 2008.

[4] M. Sivaraman and J. Sivadasan, "Comparison of pollution flashover performance of various insulators," in *Proc. Int. Conf. Circuits, Power Comput. Technol. (ICCPCT)*, Mar. 2014, pp. 148–152.

[5] X. Jiang, S. Wang, Z. Zhang, J. Hu, and Q. Hu, "Investigation of flashover voltage and non-uniform pollution correction coefficient of short samples of composite insulator intended for ±800kV UHVDC," *IEEE Trans. Dielectr. Electr. Insul.*, vol. 17, no. 1, pp. 71–80, Feb. 2010.

[6] W. Sima, T. Yuan, Q. Yang, K. Xu, and C. Sun, "Effect of Non-uniform pollution on the withstand characteristics of extra high voltage (EHV) suspension ceramic insulator string," *IET Gener., Transmiss. Distrib.*, vol. 4, no. 3, pp. 445–455, 2010.

[7] Z. Zhang, D. Zhang, J. You, J. Zhao, X. Jiang, and J. Hu, "Study on the DC flashover performance of various types of insulators with fan-shaped nonuniform pollution," *IEEE Trans. Power Del.*, vol. 30, no. 4, pp. 1871–1879, Aug. 2015.

[8] J. Seifert, W. Petrusch, and H. Janssen, "A comparison of the pollution performance of long rod and disc type HVDC insulators," *IEEE Trans. Dielectr. Electr. Insul.*, vol. 14, no. 1, pp. 125–129, Feb. 2007.

[9] R. Sundararajan and R. S. Gorur, "Effect of insulator profiles on DC flashover voltage under polluted conditions. A study using a dynamic arc model," *IEEE Trans. Dielectr. Electr. Insul.*, vol. 1, no. 1, pp. 124–132, Feb. 1994.

[10] H. Ye, J. Zhang, Y. M. Ji, W. Y. Sun, K. Kondo, and T. Imakoma, "Contamination accumulation and withstand voltage characteristics of various types of insulators," in *Proc. 7th Int. Conf. Properties Appl. Dielectr. Mater.*, 2003, pp. 1019–1023.

[11] Z. Zhang, X. Jiang, Y. Chao, L. Chen, C. Sun, and J. Hu, "Study on DC pollution flashover performance of various types of long string insulators under low atmospheric pressure conditions," *IEEE Trans. Power Del.*, vol. 25, no. 4, pp. 2132–2142, Oct. 2010.

[12] Z. Zhang, X. Jiang, C. Sun, J. Hu, and H. Huang, "Study of the influence of test methods on DC pollution flashover voltage of insulator strings and its flashover process," *IEEE Trans. Dielectr. Electr. Insul.*, vol. 17, no. 6, pp. 1787–1795, Dec. 2010.

[13] *Pollution Classification and External Insulation Selection for Electric Power System. Part II: DC System*, Standard Q/GDW 1152.2-2014, State Grid Corporation of China, Beijing, China, 2015.
[14] X. Jiang, J. Yuan, Z. Zhang, J. Hu, and L. Shu, "Study on pollution flashover performance of short samples of composite insulators intended for ±800 kV UHV DC," *IEEE Trans. Dielectr. Electr. Insul.*, vol. 14, no. 5, pp. 1192–1200, Oct. 2007.
[15] L. Yang, Y. Hao, L. Li, and Y. Zhao, "Comparison of pollution flashover performance of porcelain long rod, disc type, and composite UHVDC insulators at high altitudes," *IEEE Trans. Dielectr. Elect. Insul.*, vol. 19, no. 3, pp. 1053–1059, Jun. 2012.
[16] Y. Gu, Y. Shi, Q. Li, X. Luo, C. Xie, and L. Li, "Research on shed spacing optimization and shed parameters selection of composite post insulators for UHV DC voltage at high altitudes," in *Proc. EPTC Power Transmiss. Transformation Technol. Conf.*, 2017, pp. 1–8.
[17] Z. Zhang, "Review on DC pollution flashover characteristics of insulators," *Insulating Mater.*, vol. 50, no. 1, pp. 8–12, 2017.
[18] X. Yu, Q. Zhang, H. Yang, J. Zhou, and B. Liu, "Leakage current characteristics of long insulator string during DC pollution flashover test under various air pressures," in *Proc. Int. Conf. Condition Monit. Diagnosis (CMD)*, Sep. 2016, pp. 481–484.
[19] L. Li, Y. Gu, Y. Hao, Y. Xue, G. Xiong, L. Yang, and F. Zhang, "Shed parameters optimization of composite post insulators for UHV DC flashover voltages at high altitudes," *IEEE Trans. Dielectr. Electr. Insul.*, vol. 22, no. 1, pp. 169–176, Feb. 2015.
[20] Y. Han, L. Tang, L. Li, Q. He, Y. Hao, and S. Yao, "Influence of lightning flashover criterion on the calculated lightning withstand level of ±800 kV UHVDC transmission lines at high altitude," *IEEE Trans. Dielectr. Electr. Insul.*, vol. 22, no. 1, pp. 185–191, Feb. 2015.
[21] L. Yang, Y. Hao, L. Li, and F. Zhang, "Artificial pollution flashover performance of porcelain long rod UHVDC insulators at high altitudes," *IEEE Trans. Dielectr. Electr. Insul.*, vol. 21, no. 4, pp. 1965–1971, Aug. 2014.
[22] G. Yu, Y. Hao, and Y. Xue, "Influence of shed overhangs of composite post insulators in UHV convert stations on DC flashover performances at high altitude," *Proc. CSEE*, vol. 34, no. 15, pp. 2478–2484, 2014.
[23] C. Zhang, L. Wang, Z. Guan, and F. Zhang, "Pollution flashover performance of full-scale ±800 kV converter station post insulators at high altitude area," *IEEE Trans. Dielectr. Electr. Insul.*, vol. 20, no. 3, pp. 717–726, Jun. 2013.
[24] F. Zhang, L. Song, R. Li, G. Wang, X. Zeng, and H. Li, "Influence of the suspension modes on pollution flashover performance for-I-800 KV composite insulators under high altitudes condition," *High Voltage Eng.*, vol. 38, no. 12, pp. 3166–3170, 2012.
[25] Z. Guan, J. Li, J. Zhou, and L. Wang, "Influence of high altitude factor on the contamination flashover performance of insulators," *High Voltage Eng.*, vol. 38, no. 10, pp. 2481–2491, 2012.
[26] J. Li, J. Zhou, Z. Guan, and L. Wang, "Effects of low pressure on DC pollution performance under different insulator profiles," in *Proc. Annu. Rep. Conf. Electr. Insul. Dielectr. Phenomena*, Oct. 2012, pp. 733–736.
[27] H. Rao, L. Li, R. Li, G. Wang, Y. Liao, and F. Zhang, "Study on the external insulation performance of ±800 kV DC transmission lines at high altitudes," in *Proc. Int. Conf. High Voltage Eng. Appl.*, Sep. 2012, pp. 1–7.
[28] F. Zhang, L. Wang, Z. Guan, and M. Macalpine, "Influence of composite insulator shed design on contamination flashover performance at high altitudes," *IEEE Trans. Dielectr. Electr. Insul.*, vol. 18, no. 3, pp. 739–744, Jun. 2011.
[29] X. Jiang, Y. Chao, Z. Zhang, J. Hu, and L. Shu, "DC flashover performance and effect of sheds configuration on polluted and ice–covered composite insulators at low atmospheric pressure," *IEEE Trans. Dielectr. Electr. Insul.*, vol. 18, no. 1, pp. 97–105, Feb. 2011.
[30] J. Li, F. Zhang, Z. Guan, and L. Wang, "A study on the shed design of DC composite insulator under contamination flashover," in *Proc. Annu. Rep. Conf. Electr. Insul. Dielectr. Phenomena*, Oct. 2010, pp. 1–4.
[31] Z. Zhang, X. Jiang, C. Sun, J. Hu, and J. Yuan, "Propagation of partial arc during the DC pollution flashover process for insulator string at low air pressure," *Proc. CSEE*, vol. 29, no. 25, pp. 104–110, 2009.
[32] G. Peng, F. Zhao, Z. Guan, and L. Wang, "Study on process of DC pollution flashover of porcelain insulators of parallel double-strings form at high altitude," in *Proc. IEEE Conf. Electr. Insul. Dielectr. Phenomena*, Aug. 2009, pp. 262–265.
[33] F. Zhang, X. Wang, L. Wang, Z. Guan, H. Wen, R. Li, and Y. Ma, "Effect of arcing on DC flashover performance of contaminated porcelain insulators for various suspension patterns at high altitudes," *IEEE Trans. Dielectr. Electr. Insul.*, vol. 15, no. 3, pp. 783–791, Jun. 2008.
[34] F.-M. Zhang, H.-L. Yang, F. Zhao, L.-M. Wang, Z.-C. Guan, J. Zhou, W.-F. Li, H. Wen, and Y. Ma, "Investigation on altitude correction factor of flashover voltage of porcelain insulator for DC transmission lines," *High Voltage Eng.*, vol. 34, no. 3, pp. 451–454, 2008.
[35] J.-B. Fan, Z.-Y. Su, W.-F. Li, P. Li, and J. Zhou, "Research on profiles of HVDC post insulator and bushing," *Proc. Chin. Soc. Electr. Eng.*, vol. 27, no. 21, pp. 1–6, 2007.
[36] F. Zhang, Y. Mao, X. Wang, L. Wang, Z. Guan, H. Wen, R. Li, and Y. Ma, "Experimental investigation on flashover performance of glass insulator for DC transmission lines at high altitudes," in *Proc. Annu. Rep. Conf. Electr. Insul. Dielectr. Phenomena*, 2007, pp. 324–328.
[37] C. Sun, Y. Tian, X. Jiang, L. Shu, and W. Sima, "Flashover performance and voltage correction of iced and polluted HV insulator string at high altitude of 4000 m and above," in *Proc. 7th Int. Conf. Properties Appl. Dielectr. Mater.*, vol. 1, 2003, pp. 141–145.
[38] V. Bergman and O. Kolobova, "Some results of investigation of the dielectric strength of polluted lines insulation in reduced air-pressure conditions," *Electrotrchnika*, vol. 54, no. 2, pp. 54–56, 1983.
[39] T. Kawamura, M. Ishii, M. Akbar, and K. Nagai, "Pressure dependence of DC breakdown of contaminated insulators," *IEEE Trans. Electr. Insul.*, vols. EI-17, no. 1, pp. 39–45, Feb. 1982.
[40] X. Jiang, Z. Zhang, J. Hu, L. Shu, and C. Sun, "AC pollution flashover performance and comparison of short samples of 750 kv composite insulators with different configuration in high altitude area," *Proc. Chin. Soc. Electr. Eng.*, vol. 25, no. 12, pp. 159–164, 2005.
[41] Z. Zhang, X. Jiang, Y. Chao, C. Sun, and J. Hu, "Influence of low atmospheric pressure on AC pollution flashover performance of various types of insulators," *IEEE Trans. Dielectr. Electr. Insul.*, vol. 17, no. 2, pp. 425–433, Apr. 2010.
[42] H. P. Mercure, "Insulator pollution performance at high altitude: Major trends," *IEEE Trans. Power Del.*, vol. 4, no. 2, pp. 1461–1468, Apr. 1989.
[43] E. I. Stapenko, "Influences of air pressure and surface contamination wetting on insulation strength," *Electr. Eng.*, vol. 1, pp. 56–58, Jun. 1972.
[44] D. A. Hoch and D. A. Swift, "Flashover performance of polluted insulation: An assessment of the influence of air density," in *Proc. 3D Africon Conf.*, 1992, pp. 81–84.
[45] T. C. Cheng and H. I. M. Nour, "A study on the profile of HVDC insulators-mathematical modeling and design considerations," *IEEE Trans. Electr. Insul.*, vol. 24, no. 1, pp. 113–118, Feb. 1989.
[46] M. Fazelian, C. Y. Wu, T. C. Cheng, H. I. Nour, and L. J. Wang, "A study on the profile of HVDC insulators-DC flashover performance," *IEEE Trans. Electr. Insul.*, vol. 24, no. 1, pp. 119–125, 1989.
[47] F. A. M. Rizk and A. Q. Rezazada, "Modeling of altitude effects on AC flashover of polluted high voltage insulators," *IEEE Trans. Power Del.*, vol. 12, no. 2, pp. 810–822, Apr. 1997.
[48] *Artificial Pollution Tests on High-Voltage Insulators to be Used on A.C. Systems*, Standard IEC 507, 1991.
[49] *Artificial Pollution Tests on High-Voltage Insulators to be Used on D.C. System*, IEC 1245, 1993.
[50] Z. Renyu, G. Zhicheng, and H. Chaofeng, "Influence of low pressure on the surface pollution lightning pressure of glass plate," *Power Grid Technol.*, vol. 18, no. 3, pp. 17–21, 1994.

JIAN LI was born in Hubei, China. He received the B.Eng. degree in electrical engineering from the Huazhong University of Science and Technology, China, in 2008, and the Ph.D. degree in high voltage engineering and insulation from Tsinghua University, China, in 2013. He is currently working with Wuhan Nari Company Ltd., State Grid Electric Power Research Institute, China. His major research interests include the pollution flashover of insulators and the robot line-tracking.

ZHONG WANG was born in Hubei, China. He received the B.Eng. degree in material science and technology from the Huazhong University of Science and Technology, China, in 2008, and the Ph.D. degree in high voltage engineering and insulation from Tsinghua University, China, in 2016. He is currently working with the School of Electrical Engineering and Information, Sichuan University, China. His major research interests include the aging of insulating material, the pollution flashover of insulators, and the energy storage materials.

XIAOBO MENG was born in Henan, China, in 1986. He received the B.S. degree in electrical engineering from the Huazhong University of Science and Technology, Wuhan, China, in 2008, and the Ph.D. degree in electrical engineering from the Department of Electrical Engineering, Tsinghua University, Beijing, China, in 2013. He worked at China Southern Power Grid Corporation, from 2013 to 2020. He has been with Guangzhou University, since 2021. His research interests include the discharge behavior of outdoor insulation and overhead transmission lines.

LIMING WANG (Senior Member, IEEE) was born in Shaoxing, Zhejiang, China, in November 1963. He received the B.S., M.S., and Ph.D. degrees in high voltage engineering from the Department of Electrical Engineering, Tsinghua University, Beijing, China, in 1987, 1990, and 1993, respectively. He has been a Professor with Tsinghua University, since 2003. His major research interests include high voltage insulation and electrical discharge, flashover mechanism on contaminated insulators, and application of pulsed electric fields.